HHS Public Access

Author manuscript

*J Invest Dermatol*. Author manuscript; available in PMC 2014 July 01.

Published in final edited form as:

*J Invest Dermatol*. 2014 January ; 134(1): 24–32. doi:10.1038/jid.2013.283.

# Disrupted ectodermal organ morphogenesis in mice with a conditional histone deacetylase 1, 2 deletion in the epidermis

**Michael W. Hughes**, **Ting-Xin Jiang**, **Sung-Jan Lin**, **Yvonne Leung**, **Krzysztof Kobielak**, **Randall B. Widelitz**, and **Cheng Ming Chuong***

Department of Pathology, Keck School of Medicine, University of Southern California, Los Angeles, CA 90033

## Abstract

Histone deacetylases (HDAC) are present in the epidermal layer of the skin, outer root sheath and hair matrix. To investigate how histone acetylation affects skin morphogenesis and homeostasis, mice were generated with a *K14* promoter-mediated reduction of *Hdac1* or *Hdac2*. The skin of HDAC1 null (*K14-Cre Hdac1*$^{cKO/cKO}$) mice exhibited a spectrum of lesions including irregularly thickened interfollicular epidermis, alopecia, hair follicle dystrophy, claw dystrophy, and abnormal pigmentation. Hairs are sparse, short and intermittently coiled. The distinct pelage hair types are lost. During the first hair cycle, hairs are lost and replaced by dystrophic hair follicles with dilated infundibulae. The dystrophic hair follicle epithelium is stratified and positive for K14, involucrin, and TRP63 but negative for K10. Some dystrophic follicles are K15 positive but mature hair fiber keratins are absent. The digits form extra hyper-pigmented claws on the lateral sides. Hyper-pigmentation is observed in the interfollicular epithelium, the tail, and the feet. *Hdac1* and *Hdac2* dual transgenic mice (*K14-Cre Hdac1*$^{cKO/cKO}$ *Hdac2*$^{+/cKO}$) have similar but more obvious abnormalities. These results show that suppression of epidermal HDAC activity leads to improper ectodermal organ morphogenesis, disrupted hair follicle regeneration and homeostasis, as well as indirect effects on pigmentation.

### Keywords

follicular dystrophy; epigenetics; hair stem cells; epidermal cyst; alopecia; hairless; sebaceous gland; claws; pigmentation

## INTRODUCTION

Ectodermal organs include hairs, scales, claws, and glands. They develop and regenerate through epithelial – mesenchymal interactions mediated by molecular expression leading to morphogenetic events (Dhouailly, 1975, Chuong, 1998, Fuchs and Horsley, 2008). In these



*Author for Correspondence: Cheng-Ming Chuong, M.D., Ph.D., Department of Pathology, Univ. Southern California, HMR 315B, 2011 Zonal Ave., Los Angeles, CA 90033, Telephone: 323 442-1296, FAX: 323 442-3049, cmchuong@usc.edu.

**CONFLICT OF INTEREST**

The authors state no conflict of interest.

keratinocytes, molecular expression can be modulated by epigenetic mechanisms involving histone acetylation, methylation, phosphorylation or ubiquination (Ikegami et al, 2009, Botchkarev et al, 2012). Here we explore how histone acetylation status affects ectodermal organ homeostasis and regeneration by deleting histone deacetylase in the epidermis.

*Hdac1* encodes histone deacetylase 1 (HDAC1), an enzyme that deacetylates histones. HDAC1 is evolutionarily conserved, present in chromatin remodeling complexes, and is ubiquitously produced in all tissues (Brunmeir et al, 2009, Haberland et al, 2009). HDAC1 and HDAC2 are enriched in the basal layer of human foreskin keratinocyte raft cultures and absent in suprabasal layers (Longworth et al, 2005). Perturbing HDAC activity is associated with several abnormalities including intestinal epithelial cell differentiation (Tou et al, 2004), cardiac muscle development (Montgomery et al, 2007), pituitary gland development (Olson et al, 2006), and embryonic stem cell differentiation (Lee et al, 2007).

The functions of HDAC1 and HDAC2 were studied by conditional deletion of their enocoding genes in embryonic mouse skin (LeBoeuf et al, 2010). Mice with loss of both HDAC1 and HDAC2 activities did not have stratified epidermis nor hair follicle development. This phenotype resembles mice with TRP63 null skin (Mills et al, 1999, Candi et al, 2006). The effect of HDAC on the morphogenesis and regeneration of hair follicles in adult mouse skin remains unknown.

Our study addresses the effects of HDAC1 disruption on post-natal skin morphogenesis and homeostasis. Epithelial specific deletion of *Hdac1* (*Hdac1* $^{cKO/cKO}$) and dual *Hdac1* homozygote, *Hdac2* heterozygote (*Hdac* $^{cKO/cKO}$ *Hdac2*$^{+/cKO}$) transgenic mice were generated by expressing *Cre* from the *keratin 14* (*K14*) promoter. These two mouse lines exhibit similar skin lesions with gene dosage effects. The lesions include epidermal hyperplasia with hyperkeratosis, alopecia, dilated infundibulae, hair follicle dystrophy, cyst-like epithelial structures, claw dystrophy, and hyper-pigmentation. Immunohistochemistry (IHC) shows protein distribution patterns which suggest that epidermal HDAC1 and HDAC 2 are involved in hair follicle regeneration. Without proper HDAC1 function, epithelial cell differentiation in affected ectodermal organs is perturbed. This work illustrates the importance of epigenetic processes in the development and regeneration of skin and its appendages.

## RESULTS

### Endogenous HDAC1 protein distribution in the epidermis of mouse skin and hair follicles

HDAC1 is enriched in the basal epidermal layer and decreases in differentiated suprabasal layers in wild type mice skin (Supplementary Figure S1a, a’ online). Whole mount HDAC1 IHC of dorsal skin demonstrates suprabasal keratinocyte nuclei are HDAC1 negative (Supplementary Figure S1a’ online). In hair follicles, HDAC1 is strongly present in the outer root sheath (ORS) and matrix, weakly in the inner root sheath (IRS) and is undetectable in the medulla (Supplementary Figure S1b, c, e online). It also is present in the sebaceous glands of anagen hair follicles (Supplementary Figure S1a–d online).

### *K14-Cre Hdac1*$^{cKO/cKO}$ mice were generated to explore the function of HDAC in ectodermal organ formation and regeneration

Since HDAC1 functionally null mice are embryonic lethal (Lagger et al, 2002), tissue specific transgenic mice were generated. K14 was used to direct Cre recombinase to the skin epithelium. K14-Cre mice were bred with *Hdac1loxp* or *Hdac1loxP Hdac2loxP* mice to generate *Hdac1*$^{cKO/cKO}$ and *Hdac1*$^{cKO/cKO}$ *Hdac2*$^{+/cKO}$ mice, respectively. This removed mouse *Hdac1* exons 5, 6, and 7 (Supplementary Figure S2 online; adapted from Montgomery 2007) in *Hdac1*$^{cKO/cKO}$ as well as exons 2, 3, and 4 of the *Hdac2* gene in *Hdac1*$^{cKO/cKO}$ *Hdac2*$^{+/cKO}$ mice (not shown). Polymerase chain reaction amplification of *Hdac1*, *Hdac2* and *Cre* demonstrate that mouse A is *Hdac1*$^{+/cKO}$ *Hdac2*$^{cKO/cKO}$, mouse B is *Hdac1*$^{cKO/cKO}$ *Hdac2*$^{+/cKO}$, and mice C and D are *Hdac1*$^{+/cKO}$ *Hdac2*$^{+/cKO}$ (Supplementary Figure S2b online). Mouse genotypes confirmed that all mice with a phenotype possessed the recombined *Hdac1* allele (Supplementary Figure S2c online). Mice with suppressed HDAC1 activity (HDAC1$^{-}$) increased epithelial cell histone 4 (H4) acetylation (Supplementary Figure S5 online).

### HDAC1 null mice have gross ectodermal pathologies

Since Cre-mediated excision of *Hdac1* was driven by a *K14* promoter, defects were noted at many different sites. The pathology at each site is discussed.

**Alopecia and abnormal hair morphology—**At 6 months, HDAC1$^{-}$ mice were smaller than their wild type littermates (Figure 1a, Supplementary Figure S3 online). Adult HDAC1$^{-}$ mouse dorsal skin exhibited extensive alopecia, abnormal and twisted hair fibers, hyperkeratosis, dilated infundibulae, hair follicle dystrophy, and epithelial cyst-like structures (Figure 1a, 1b). This phenotype was less evident at 9 days. Alopecia appeared during the first hair cycle and did not progress to open lesions, ulcers, or scarring. To evaluate subcutaneous hair follicle morphology, the underlying skin of wild type mice was revealed by shaving (Figure 1b1); however, shaving was unnecessary on HDAC1$^{-}$ mice as their abnormal hairs were sparse (Figure 1b2). Examining HDAC1$^{-}$ dorsal skin from the dermal side (Figure 1b4) revealed hair follicle dystrophy, ingrown hair fibers, coiled hair follicles and disrupted hair follicle alignment (Figure 1b6) compared to wild type skin (Figure 1b3 and b5).

Wild type mice exhibit 4 types of pelage hairs; guard, awl, auchen, and zigzag (Schmidt-Ullrich et al, 2006); whereas affected follicles of HDAC1$^{-}$ mice have only one hair type resembling abnormal zigzag hair (Figure 1c). Hair follicle orientation was abnormal with fibers pointing towards the dermis instead of toward the epithelium (Figure 1b6). The hair medulla was abnormal with misaligned air cells (Figure 1c).

**Abnormal appearance in facial ectoderm—**The HDAC1$^{-}$ mice had enlarged eyelids and smaller eye openings (Figure 1d) (The white corneas are artifacts). The periorbital area showed normal cilia (eyelashes) but pelage hair numbers were reduced and the hair pattern was disrupted (Figure 1d). Vibrissa hair fiber thickness and length were reduced in the HDAC1$^{-}$ mice (Figure 1d and data not shown). These abnormalities were more severe in *K14-Cre Hdac1*$^{cKO/cKO}$ *Hdac2*$^{+/cKO}$ mice (Figure 1d). These mice are designated HDAC1,

2⁻. The Meibomian glands exhibited hyperplasia (Supplementary Figure S4m online, black brackets).

**Paws exhibit supernumerary claws—**Foot skin epithelium was hyperkeratotic (Figure 1f, g). Pigmentation was increased in the claws, footpads, and feet. Claw dystrophies included unique outgrowths of the hyponychium that greatly extended beyond the claw matrix. Extra (supernumerary) claws formed on the lateral sides of digits (Figure 1g). Supernumerary claw matrices were covered with compact keratin structures extending from the proximal claw fold (Figure 1e, green box in Figure 1g, plane of section in Figure 1e). Hyper-pigmentation was due to the presence of ectopic pigmented melanocytes at the dermal-epidermal junction in the claw matrix (Figure 1e green arrow). HDAC1, 2⁻ mice showed more severe pigmentation and supernumerary claw phenotypes (Figure 1f, g). Sweat gland histology and IHC for K5 (duct and gland basal epithelial layer) and K8 (gland luminal epithelial layer) was normal in HDAC1⁻ compared to wild type mouse footpads (Supplementary Figure S4j, k online).

## Progressive development of dystrophic hair follicle cysts

**Hair appeared normal at postnatal day 9—**The skin of 9 day old HDAC1⁻ mice did not exhibit a prominent phenotype (Figure 2a). All of the pelage hair types; guard, awl, auchene and zigzag were present (not shown).

***Dystrophic hair follicle cysts began to form by 3 weeks*** (first hair cycle onset) (Figure 2b′ boxed region in 2b; b–d). At this time, some hair follicles appeared to be in transitional stages between normal and dystrophic follicles. In one example, a relatively normal club hair is above a disorganized matrix region with a dilated infundibulum (Figure 2e, green bracket). Another example shows an abnormal follicle whose dermal papilla (DP) is connected by an epithelial stalk to disorganized matrix (Figure 2h). This opened into an enlarged infundibulum filled with cornified material (Figure 2h, black asterisk). Alkaline phosphatase (AP) staining, a DP marker, was observed at the proximal end of these transitional stage follicles (Figure 2g, h).

**Dystrophic hair follicle cysts became prevalent by 3 months—**At this time, dystrophic follicles increased in number but their epithelia had similar characteristics as those found at 3 weeks. For instance, the range of Keratin 14 (K14) and cell envelope protein involucrin (IVL) expanded from the basal to innermost epithelial layers (Figure 2f, f′, j, 3 left column). IHC for keratin 10 (K10), a suprabasal skin epithelium differentiation marker (Figure 2i), was negative at 3 weeks and at later times (Supplementary Figure S4c online). TRP63, a basal epithelial cell transcription factor that modulates epithelial stratification, was present in the dystrophic follicular epithelia (Figure 2k, 3 left column).

**Conversion to dystrophic hair follicle cysts was nearly complete at 6 months—**Histological analysis of 6 month HDAC1⁻ mice exhibited moderate epidermal hyperplasia and hyperkeratosis (Figure 3 right column, Supplementary Figure S4a). Generally, the trend of differentiation from the basal layer toward the stratum corneum was preserved (Figure 3 right column, Supplementary Figure S4a). However, keratinocytes in all

layers were highly variable in cell size and shape (Supplementary Figure S4a online). The prevalence of hair follicle dystrophy was similar for mice at 3 and 6 months (Figure 3, H&E). The enlarged infundibula of dystrophic follicles sometimes contained keratin arranged in columns resembling a hair shaft and others contained keratin with less structure (Figure 3, H&E). Dystrophic follicular epithelium was often stratified without a significant granular layer (Figure 3, H&E).

**Characterization of dystrophic follicle cysts showed they formed from hair follicle progenitor cells that failed to differentiate properly—**Cell dynamics and differentiation were further examined in the interfollicular skin of 6 month HDAC1$^{-}$ mice (Figure 3, Supplementary Figure S4 online). Proliferating cells were present in the cysts. TUNEL staining, a measure of apoptosis, was increased in the epidermal basal layer compared to controls (data not shown and Supplementary Figure S4f online). In interfollicular epithelia, K14 (Figure 3 right column, Supplementary Figure S4b online) and K10 (Supplementary Figure S4c online) staining was expanded to additional layers. TRP63 exhibited a normal distribution pattern (Figure 3 right column).

In the dystrophic hair follicles, K14 was positive from the basal to the innermost epithelial layer (Supplementary Figure S4b online). K10 (Supplementary Figure S4c online) and LEF1 (Supplementary Figure S4d online) were absent from the abnormal follicle epithelium. AE13 (Supplementary Figure S4e online) also were negative in dystrophic hair follicles. IVL was distributed across all epithelial cyst layers (Figure 3 right column). TUNEL staining was positive in the cyst epithelium (Supplementary Figure S4f online). The activated bulge stem cell marker, CD200 (Supplementary Figure S4g online), was greatly reduced or absent. Dystrophic follicles showed increased staining for K15, a hair follicle stem cell marker (Supplementary Figure S4h online). β-catenin (Supplementary Figure S4i online) and TRP63 (Figure 3 right column) were present throughout the dystrophic hair follicle epithelia. Collectively, these data suggest that hair differentiation was disrupted in K14 producing keratinocytes; epidermal differentiation was maintained but control of homeostasis was disrupted.

**Tail skin showed hyperplastic epidermis, a non-autonomous increase of pigment cells, and an increase of lipid retaining cells—**The tail skin exhibited several pathological features (Figure 2l–q). Wild type tail interfollicular epidermis was pigmented and the hair follicles (yellow outline) were highly organized (Figure 2l, l′). Pigmentation was restricted to the pilosebaceous units, and localized to the scale or perifollicular region (Figure 2l**********′). The HDAC1$^{-}$ mouse tail (Figure 2m, m′, n, n′) exhibited hyperkeratosis, hyper-pigmentation, and a reduction in normal hair compared to wild type. In HDAC1$^{-}$ mice pigmentation and melanocytes expanded into the region between scales (Figure 2m′, n′). IHC for microphthalmia-associated transcription factor (Mitf) demonstrated an increased number of melanoblasts in the HDAC1$^{-}$ mice inter-scale region compared to wild type mice (Supplementary Figure S4l online). Lipid retaining cells, assessed by Oil Red O staining, increased in a gene dose-dependent manner in tail hair follicles and sebaceous glands (Figure 2o–q).

## DISCUSSION

This study characterizes the endogenous distribution of HDAC1 and examines the effects of HDAC1 disruption on adult mouse skin (Figure 4). These mice exhibited phenotypes in multiple anatomical regions (Figure 4). The overall body size was decreased compared to wild type mice. The *K14* promoter used to drive Cre excision of *Hdac1* was expressed in the basal epithelium which affected various tissues in different areas, including the teeth, claws, and upper esophagus. It is not surprising that a lack of HDAC1 in the upper esophagus might lead to malnutrition which would produce a smaller mouse.

### Defective morphogenesis and differentiation in the ectodermal organs of HDAC1$^{-}$ adult mice

Normal adult mouse skin contains interfollicular epidermis with well defined basal and suprabasal layers including pilosebaeous units with ORS, IRS, hair matrix, and sebaceous glands. Homozygous HDAC1 disruption led to abnormal skin morphogenesis (Figure 4a). HDAC1$^{-}$ mouse skin architecture was generally preserved but the epidermis was thickened and hyperkeratotic. Epithelial apoptosis was increased. A comparison of HDAC1$^{-}$ with HDAC1, 2$^{-}$ mice showed a gene dose-dependence in phenotype severity. A single heterozygous mutation of either *Hdac1* or *Hdac2* exhibited no phenotype. This suggests that HDAC1 and HDAC2 partially compensate for each other.

Hair follicle morphogenesis was observed but the characteristic hair types were replaced by abnormally pigmented, shorter, thinner hairs with misshaped and twisted medulla structures. Subsequent hair cycles produced dystrophic hair follicles with dilated infundibula (Figure 4b) demonstrating that the differentiation of hair follicle progenitor cells was perturbed. Normal epithelial-mesenchymal interactions necessary for DP homeostasis may be disrupted because the DP cells appeared to disperse. Analysis of hair follicle differentiation did not detect molecules normally present in the matrix (LEF1), inner root sheath (AE15), medulla (AE15), or hair shaft (AE13). Furthermore, the expanded K14 and K15 distribution domains in dystrophic hair follicles imply cells abnormally retain a primitive undifferentiated state in both interfollicular and follicular regions. Hair follicle regeneration requires activation of hair stem cells, lineage specifying progenitor cells, and functional matrix cells for hair filament differentiation. However, since HDAC1 is normally enriched in these cell types and is missing in HDAC1$^{-}$ mutants, all of these cell lineages may be affected. Our current data on adult hair follicle regeneration implies HDAC1$^{-}$ mice may be defective in specifying cells toward hair lineage differentiation. Future studies on the downstream mechanism will help identify which components contribute to follicular dystrophy.

HDAC1$^{-}$ mice showed changes in pigmentation. Whole mount IHC patterns of Mitf, a melanocyte differentiation marker, demonstrated increased numbers of melanoblasts in the HDAC1$^{-}$ mice. If HDAC1 was specifically deleted in keratinocytes and not melanocytes, then our finding suggests that depletion of HDAC activity in the epidermis can non-autonomously affect the number of melanocyte progenitors by increasing either their recruitment or proliferation into normally unpigmented areas. Although increased melanocyte cell proliferation was not observed at the time points examined, this may occur

during development. The effect of HDAC on melanocyte biology will be addressed in future studies.

Although younger HDAC1$^{-}$ mice (Figure 2) exhibited less hair follicle dystrophy than older mice (Figure 3), their IHC patterns suggest the dystrophy may be a progressive pathological change due to a common etiology.

## Context-dependent effects of HDAC

HDAC1 and HDAC2 have overlapping patterns during development and tissue homeostasis. They compensate for one another *in vitro* but have distinct gene modulation functions *in vivo* (Brunmeir et al, 2009, Haberland et al, 2009). The role of HDAC1 and HDAC2 in skin and hair follicle development was previously explored utilizing HDAC1, 2 functionally null skin during mouse development (LeBoeuf et al, 2010). K14-Cre Hdac1$^{fl/fl}$ Hdac2$^{fl/fl}$ (dcKO) mice were embryonic lethal around E18.5 to E19 due to a failure in skin morphogenesis. H3K9 acetylation levels were elevated in embryonic dcKO mouse skin (Supplementary Table S1 online). At a gross level, embryonic dcKO mice did not display epidermal stratification, hair follicle initiation, eyelid fusion, nor digit separation. These mice did display tooth defects. From these abnormalities and molecular data, the authors suggest that skin appendage development may be blocked at an early stage. At the cellular level, a progressive loss of proliferation suggests that progenitor cells are not maintained and a concomitant progressive increase in apoptosis exacerbates the defects. The authors noted that the dcKO phenotype was similar to TRP63 mutants.

Our study focused on postnatal defects in skin development and compared molecular marker distributions between embryonic dcKO (Leboeuf et al, 2010) and adult HDAC1$^{-}$ mice (Supplementary Table S1 online). Whereas PCNA staining was decreased in embryonic dcKO mouse skin, it was increased in adult HDAC1, 2$^{-}$ epithelium (Supplementary Table S1 online). Since embryonic skin development and adult hair follicle epithelium homeostasis are biologically different processes, these seemingly contradictory results may imply these stages have different epigenetic landscapes. Interestingly, TUNEL staining was increased in adult HDAC1, 2$^{-}$ mouse skin epithelium and is consistent with E16.5 dcKO mouse skin. Abnormal cell cycle regulation leads to apoptosis. No viable HDAC1, HDAC2 homozygote functionally null mice were observed in our study because the dcKO was probably embryonic lethal (LeBoeuf et al, 2010).

Although LeBoeuf (et al., 2010) reported no skin phenotype in adult HDAC12$^{-}$ mice, they now observe a skin phenotype in inducible Cre-lox adult mice (personal communication). Background strains have been known to affect phenotypes. A possible reason for the discrepant results is C57BL/6J mice were used in our study and LeBoeuf (et al, 2010) used a multiple background strain.

## Epithelial cysts from K14-Cre(neo); β-cat lox/null mice

Cyst formation was previously observed in K14-cre β-catenin$^{fl/fl}$ mice (Huelsken et al, 2001) which lack embryonic hair formation. During the first hair cycle, hairs in β-catenin positive skin were replaced by cysts. These cysts were positive for K10 and IVL in the innermost

epithelial layers and lacked sebaceous glands. HDAC1$^{-}$ mice also form cysts and show elevated IVL staining levels. However, these mice exhibit sebaceous hyperplasia, expanded K14 and K15, and no K10 staining in epithelial cysts. HDAC1$^{-}$ mice have high β-catenin levels in the cyst epithelium (Figure 4i), suggesting HDAC1$^{-}$ epithelial cysts are different than those found in K14-Cre β-catenin$^{fl/fl}$ mice.

Cysts have been observed when other complex epithelial organs fail to form properly. For example, in polycystic kidney disease primary cilia are defective. Patients who suffer from Birt–Hogg–Dubé syndrome develop lung, skin, and kidney cysts (Hartman et al, 2009). Similarly, hair follicle dystrophy development may be the default outcome of improper morphogenesis. Complex tissues and their respective organs will not form if molecular signaling cascades are abnormal or tissue competency is compromised (Figure 4c).

HDAC1$^{-}$ mice provide an animal model in which the roles of histone acetylation in the development, regeneration and pathology of ectodermal organs can be studied further. Our future directions include characterizing downstream molecular targets and cellular mechanisms leading to the observed pathology.

## MATERIALS AND METHODS

### Transgenic mice

C57BL/6J or HDAC1$^{-}$ or HDAC1, 2$^{-}$ *mice*

C57BL/6J mice were purchased from Jackson Laboratories (Bar Harbor, Maine). The K14-Cre mice, a gift from Dr. Yang Chai's lab at USC, were described previously (Hosokawa et al, 2009). The Hdac1loxp and Hdac2loxp mice, a gift of Eric Olson (UTSW), were described previously (Montgomery et al, 2007). K14-Cre mice were bred with Hdac1loxp and/or Hdac2loxp mice to generate HDAC1$^{-}$ and HDAC1, 2$^{-}$ mice. Mice were genotyped as previously described (Montgomery et al, 2007). All mice reported in this study are male, range in age from 9 days to 6 months, and are disease-free. All animal studies were approved by the University of Southern California Institutional Animal Care and Use Committee.

### Histology and Immunostaining

Paraffin section IHC (Jiang et al, 1998) and whole mount IHC (Ito et al, 2007) were performed using the following antibodies; K14 (Lab Vision Cat.# MS-115), K10 (Lab Vision Cat.# MS-611), CTNNB1 (β-catenin Sigma Cat.# C2206), PCNA (Chemicon Cat.# CBL407), TRP63 (p63, Santa Cruz Cat.# SC-8343), IVL (Involucrin, Lab Vision Cat.# MS-126), K15 (Lab Vision Cat.# MS-1068), LEF1(Abcam Cat.# ab22884), CD200 (R&D Cat.# AF3355), SOX2 (R&D Cat.# AF2018), NCAM1 (Chuong and Edelman, 1985), AE13 (Santa Cruz Cat.# SC-57012), TCHH (AE15 Santa Cruz Cat.# SC-98968) and HDAC1 (Lab Vision Cat.# RB-9223). K5 (a gift from Dr. Collin Jamora, UC San Diego) and K8 (TROMA-I, Developmental Studies Hybridoma Bank, University of Iowa, Iowa City, IA). Color was developed with the AEC kit (Vector Labs) or visualized with fluorescent secondary antibodies.

For whole mount Oil Red O staining, mouse skin was incubated in 20mM EDTA at 37°C until the epithelium separated from the mesenchyme. The epithelium was fixed in 4% PFA (paraformaldehyde) for 30 min at room temperature, immersed in Propylene Glycol for 10 min, in Oil Red O Solution (0.7gm Oil Red O in 85% Propylene Glycol and $dH_2O$) for 1 hr at room temperature, and rinsed in $dH_2O$ for visualization.

### Confocal microscopy

A confocal microscope (LS510, Carl Zeiss) was used to image fluorescently (Alexa, Invitrogen) labeled cells and nuclei. Z stack images were captured and processed in the LSM Image Browser software (Carl Zeiss).

## Supplementary Material

Refer to Web version on PubMed Central for supplementary material.

## Acknowledgments

This research was supported by the NIH NIAMS through grants AR 42177 (CMC), AR 47364 (CMC, RW), and AR 60306 (CMC). KK and YL are supported by RO3 AR 061028. Dr. SJ Lin is supported by a fellowship from NHRI, Taiwan. We thank Dr. E. Olson for the *Hdac1loxp* and *Hdac2loxp* mice. Confocal microscopy was performed in the Cell and Tissue Imaging Core of the USC Research Center for Liver Diseases, NIH grant No. P30DK048522. Procedures for all animals utilized in this study were approved by the University of Southern California Institutional Animal Care and Use Committee.

## Abbreviations

| | |
|---|---|
| **HDAC** | Histone Deacetylase |
| **cKO** | conditional knockout |
| **K** | keratin |
| **IHC** | immunohistochemistry |

## References

Botchkarev VA, Gdula MR, Mardaryev AN, et al. Epigenetic regulation of gene expression in keratinocytes. J Invest Dermatol. 2012; 132:2505–21. [PubMed: 22763788]

Brunmeir R, Lagger S, Seiser C. Histone deacetylase HDAC1/HDAC2-controlled embryonic development and cell differentiation. Int J Dev Biol. 2009; 53:275–89. [PubMed: 19412887]

Candi E, Rufini A, Terrinoni A, et al. Differential roles of p63 isoforms in epidermal development: Selective genetic complementation in p63 null mice. Cell Death Differ. 2006; 13:1037–47. [PubMed: 16601749]

Chuong, CM., editor. Molecular basis of epithelial appendage morphogenesis. Landes Bioscience; Austin, TX: 1998. p. 444

Chuong CM, Edelman GM. Expression of cell-adhesion molecules in embryonic induction. I. morphogenesis of nestling feathers. J Cell Biol. 1985; 101:1009–26. [PubMed: 3897241]

Dhouailly D. Formation of cutaneous appendages in dermo-epidermal recombinations between reptiles, birds and mammals. Wilhelm Roux' Arch Entwicklungsmech Org. 1975; 177:323–40.

Fuchs E, Horsley V. More than one way to skin. Genes Dev. 2008; 22:976–85. [PubMed: 18413712]

Haberland M, Montgomery RL, Olson EN. The many roles of histone deacetylases in development and physiology: Implications for disease and therapy. Nat Rev Genet. 2009; 10:32–42. [PubMed: 19065135]

Hartman TR, Nicolas E, Klein-Szanto A, et al. The role of the birt-hogg-dube protein in mTOR activation and renal tumorigenesis. Oncogene. 2009; 28:1594–604. [PubMed: 19234517]

Hosokawa R, Deng X, Takamori K, et al. Epithelial-specific requirement of FGFR2 signaling during tooth and palate development. J Exp Zool B Mol Dev Evol. 2009; 312B:343–50. [PubMed: 19235875]

Huelsken J, Vogel R, Erdmann B, et al. Beta-catenin controls hair follicle morphogenesis and stem cell differentiation in the skin. Cell. 2001; 105:533–45. [PubMed: 11371349]

Ikegami K, Ohgane J, Tanaka S, et al. Interplay between DNA methylation, histone modification and chromatin remodeling in stem cells and during development. Int J Dev Biol. 2009; 53:203–14. [PubMed: 19412882]

Ito M, Yang Z, Andl T, et al. Wnt-dependent de novo hair follicle regeneration in adult mouse skin after wounding. Nature. 2007; 447:316–20. [PubMed: 17507982]

Jiang, TX.; Stott, S.; Widelitz, RB., et al. Current methods in the study of avian skin appendages. In: Chuong, CM., editor. In Molecular basis of epithelial appendage morphogenesis. Landes Bioscience; Austin, TX: 1998. p. 359-408.

Lagger G, O'Carroll D, Rembold M, et al. Essential function of histone deacetylase 1 in proliferation control and CDK inhibitor repression. EMBO J. 2002; 21:2672–81. [PubMed: 12032080]

LeBoeuf M, Terrell A, Trivedi S, et al. Hdac1 and Hdac2 act redundantly to control p63 and p53 functions in epidermal progenitor cells. Dev Cell. 2010; 19:807–18. [PubMed: 21093383]

Lee ER, Murdoch FE, Fritsch MK. High histone acetylation and decreased polycomb repressive complex 2 member levels regulate gene specific transcriptional changes during early embryonic stem cell differentiation induced by retinoic acid. Stem Cells. 2007; 25:2191–9. [PubMed: 17525233]

Longworth MS, Wilson R, Laimins LA. HPV31 E7 facilitates replication by activating E2F2 transcription through its interaction with HDACs. EMBO J. 2005; 24:1821–30. [PubMed: 15861133]

Mills AA, Zheng B, Wang XJ, et al. P63 is a P53 homologue required for limb and epidermal morphogenesis. Nature. 1999; 398:708–13. [PubMed: 10227293]

Montgomery RL, Davis CA, Potthoff MJ, et al. Histone deacetylases 1 and 2 redundantly regulate cardiac morphogenesis, growth, and contractility. Genes Dev. 2007; 21:1790–802. [PubMed: 17639084]

Olson LE, Tollkuhn J, Scafoglio C, et al. Homeodomain-mediated beta-catenin-dependent switching events dictate cell-lineage determination. Cell. 2006; 125:593–605. [PubMed: 16678101]

Schmidt-Ullrich R, Tobin DJ, Lenhard D, et al. NF-kappaB transmits eda A1/EdaR signalling to activate shh and cyclin D1 expression, and controls post-initiation hair placode down growth. Development. 2006; 133:1045–57. [PubMed: 16481354]

Tou L, Liu Q, Shivdasani RA. Regulation of mammalian epithelial differentiation and intestine development by class I histone deacetylases. Mol Cell Biol. 2004; 24:3132–9. [PubMed: 15060137]

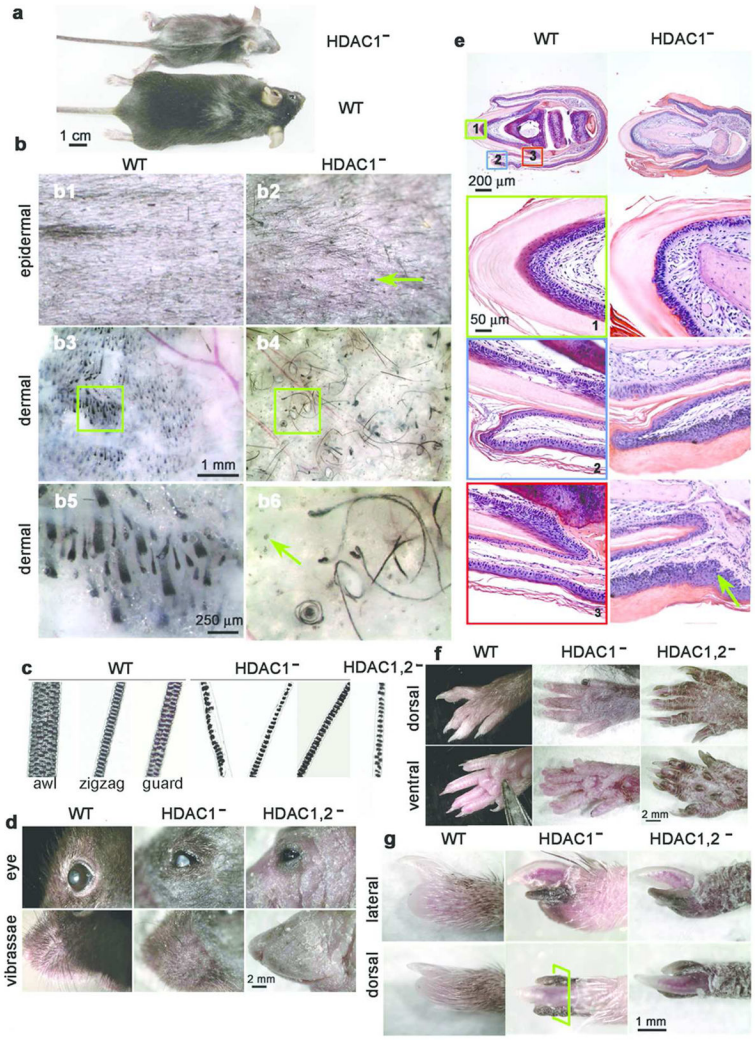


**Figure 1. Multiple skin ectodermal organs show abnormal morphology in HDAC1⁻ mice**

a) Adult HDAC1⁻ mice are smaller and develop alopecia. b) Dorsal skin of wild type (b1) versus HDAC1⁻ (b2) mice with pigmented cysts (green arrows). View from the dermal side of HDAC1⁻ skin (b3 and b4) shows abnormal hair patterning, ingrown hairs, and follicular dystrophy (boxes, magnified areas in b5 and b6). c) Abnormal HDAC1⁻ mouse hair fiber types. d) Normal hair follicles and eye openings are reduced. Vibrissae are abnormal and interfollicular epithelium is hyper-pigmented. e) H&E staining shows melanocytes are present at the dermal-epidermal junction of the claw (green arrow) in HDAC1⁻ mice. f) Feet exhibit hyperkeratosis and hyper-pigmentation. g) Supernumerary pigmented claws (green box, plane of section for panel e). a, scale bar = 1 cm; b3–b4, g, scale bar = 1mm; b5–b6, scale bar = 250 µm; d, f, scale bar = 2 mm; e, 200 µm, e1–3 scale bar = 50 µm.

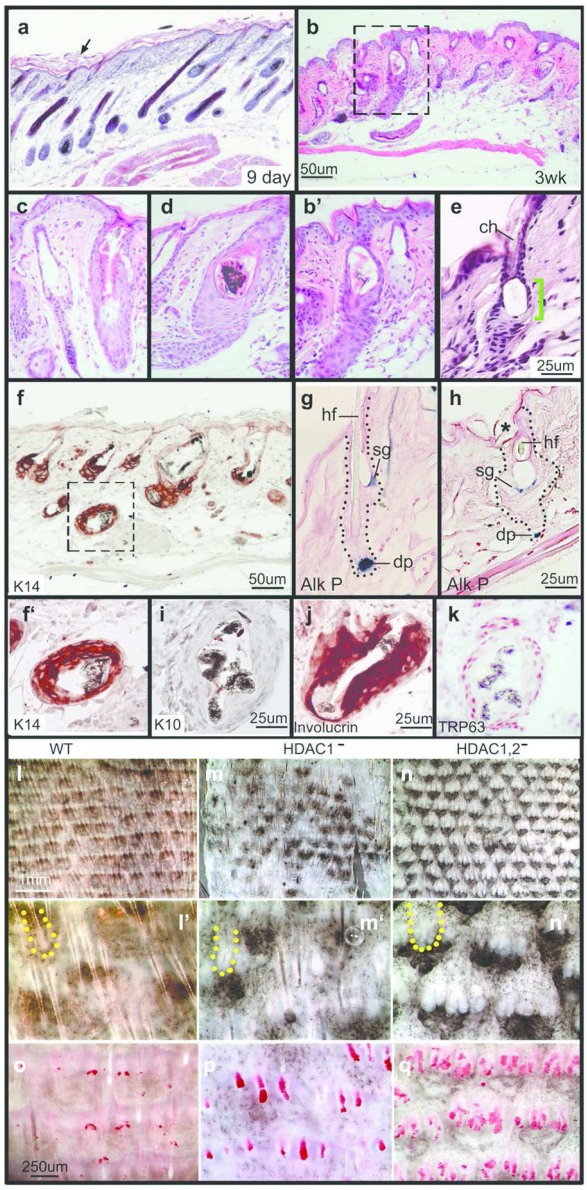


**Figure 2. Hairs appear normal in newborn but alopecia and dystrophic changes occur at the first hair cycle**

a–e) H&E staining of a) 9 day vs b) 3 week cKO skin (black arrow, hyperkeratosis. Scale bar = box, magnified view in panel b′). c–e) Dystrophic follicles (ch, club hair; green bracket, initial dystrophic change). f) K14 (box, magnified view in f′) and g, h) alkaline phosphatase distribution in dystrophic follicles (sg, sebaceous glands; dp, dermal papilla; dotted line, abnormal follicle; black asterisk, infundibulum; hf, hair fiber). i) K10 is negative, while j) IVL and k) TRP63 are positive in dystrophic follicles. l-n, l′-n′) The tail pigmentation in 6 month wild type or HDAC1⁻ mice. o–q) Oil Red O staining of wild type or HDAC1⁻ tail hair follicles. a, b, f, scale bar = 50 μm; b′, c–e, f′, g–k, scale bar = 25 μm; l-n scale bar = 1 mm; l′-n′, o–q, scale bar = 250 μm.

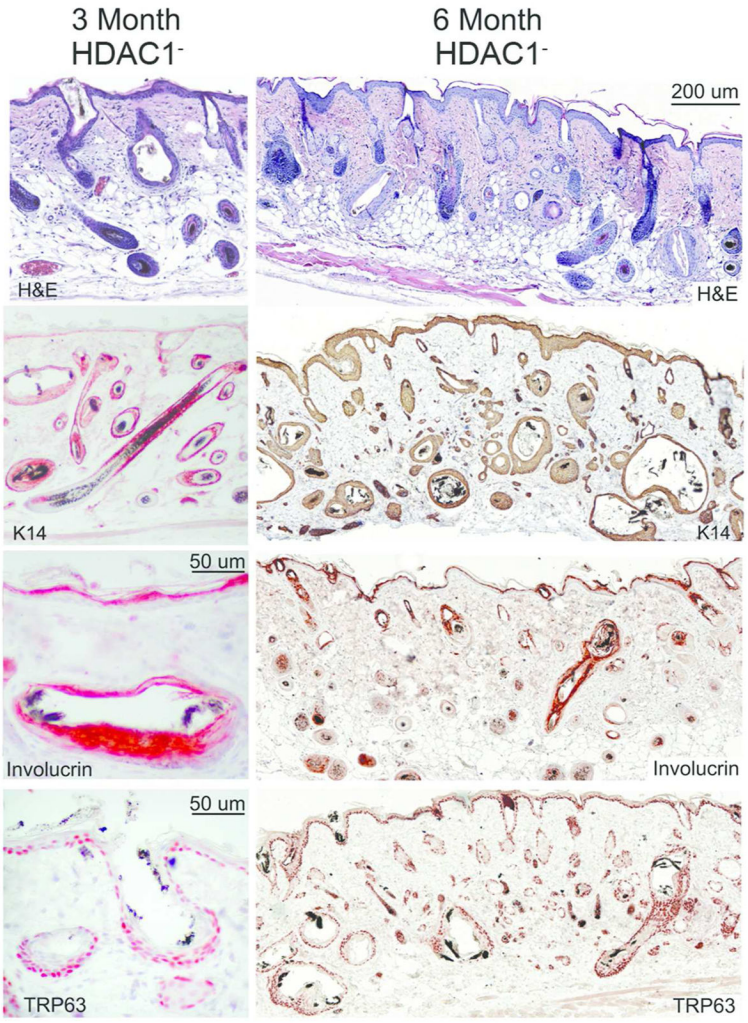


**Figure 3. Dystrophic hair follicle cysts are pronounced in 3 and 6 month HDAC1⁻ mice**

Histology demonstrates hyperkeratosis, fewer normal follicles, follicular dystrophy, widened infundibula and thicker inter-follicular epidermis in HDAC1⁻ mouse skin at 3 (left column) and 6 (right column) months. These lesions are increased in number in the 6 month HDAC1⁻ mice. At both time points, the basal marker K14 is increased, expands beyond the basal epithelial layer, and is present in the epithelial wall of dystrophic hair follicles. IVL is strongly positive in the infundibulae and dystrophic follicles. TRP63 staining is normal in the basal layer and is present in the cyst wall epithelia. Left column (H&E, K14), right column, scale bar = 200 μm; left column (Involucrin, TRP63), scale bar = 50 μm.

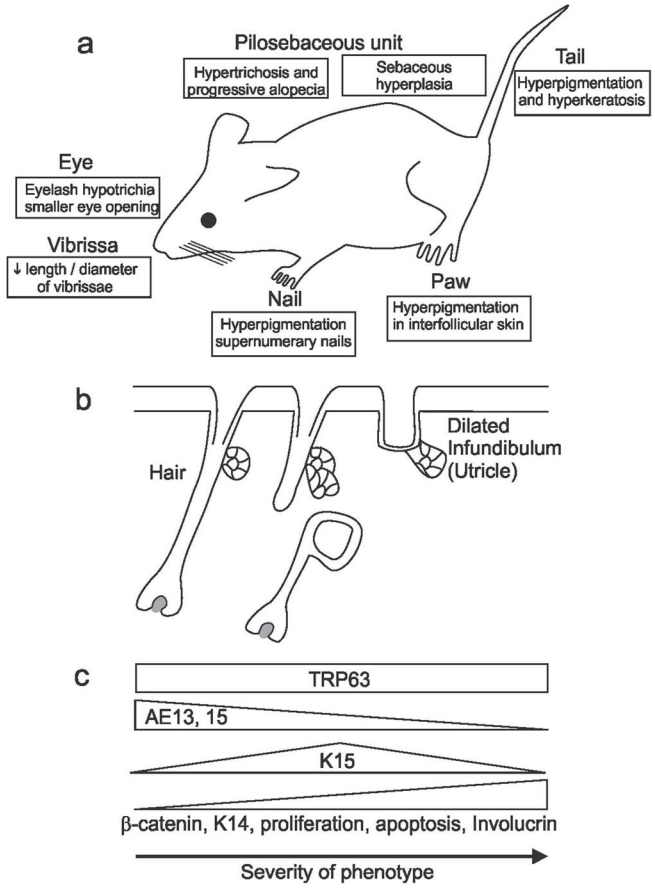


**Figure 4. Summary of the effect of HDAC1 loss in mouse skin ectodermal organs**

a) Schematic highlighting phenotypic alterations of ectodermal organs found at different anatomic locations in the mouse. b) The range of skin phenotypes from normal to dystrophic follicles with cyst-like phenotypes is shown. c) Schematic representation of altered molecular expression in the skin and hair follicle dystrophy of HDAC mutants as they mature from 3 weeks to 3 months, and finally to 6 months.